ITRF2008 contribution to glacial isostatic adjustment and recent ice melting assessment

Laurent Métivier, Xavier Collilieux, Zuheir Altamimi

ITRF2008 contribution to glacial isostatic adjustment and recent ice melting assessment

Laurent Métivier,[1,2] Xavier Collilieux,[1] and Zuheir Altamimi[1]

Received 10 October 2011; revised 30 November 2011; accepted 30 November 2011; published 14 January 2012.

[1] We investigate what information station vertical velocities of the ITRF2008 provide on global geodetic parameters and by extension on glacial isostatic adjustment (GIA) and recent ice melting (RIM) processes. We infer degree-2 spherical harmonic coefficients (SHC) of the Earth figure change and the J_2 gravity rate ($\dot{J}_2$), which we compare with five GIA models. We find $\dot{J}_2$ to be (0.0 ± 2.4) × 10^{-11} yr^{-1}, which is consistent with recent studies that propose a $\dot{J}_2$ change in the 1990s, due to RIM whose contribution to the $\dot{J}_2$ would be today around (3.5–4.0 ± 2.4) × 10^{-11} yr^{-1}. Such results favor Peltier (2004) VM2 or Paulson et al. (2007) GIA models. The ITRF2008 SHC that are directly impacted by the GIA rotational feedback, confirm with a good precision recent results from GRACE mission that initiated a debate on GIA rotational feedback and about Peltier GIA model quality. We find a coefficient consistent with Paulson's (and other) model and more than 7 times smaller than coefficients in Peltier's models. Two explanations are possible: (1) if the model of Peltier (2004) VM2 were to be correct, then the strong rotational feedback in the model must be counteracted by a strong rotational feedback in the opposite direction generated by current ice loss, (2) if the model of Paulson et al. (2007) were to be correct, therefore GIA and RIM separately induce negligible rotational feedbacks. Both answers are quite extreme and call for more investigation on GIA modeling and rotational feedback. **Citation:** Métivier, L., X. Collilieux, and Z. Altamimi (2012), ITRF2008 contribution to glacial isostatic adjustment and recent ice melting assessment, *Geophys. Res. Lett.*, *39*, L01309, doi:10.1029/2011GL049942.

1. Introduction

[2] The glacial isostatic adjustment (GIA) is due to the unloading of ice on the Earth surface following the last deglaciation period, a few thousand years ago. The ice mass redistributions induce an adjustment of the planet. Following this adjustment, there are viscoelastic deformations of the solid Earth [e.g., *Peltier*, 1974; *Mitrovica et al.*, 1994], sea level rise [e.g., *Peltier*, 1998], gravity variations, geocenter motions [*Greff-Lefftz*, 2000; *Argus*, 2007; *Greff-Lefftz et al.*, 2010; *Métivier et al.*, 2010, 2011], and also disruption of the Earth's rotation ("true polar wander") [e.g., *Mitrovica et al.*, 2005; *Peltier and Luthcke*, 2009]. ICE5G-VM2 model from *Peltier* [2004] is generally considered as the reference in terms of GIA processes. But a recent study from *Chambers et al.* [2010] suggests that Peltier GIA model is not consistent with sea level rise and gravity observations inferred from the GRACE gravity space mission [*Tapley et al.*, 2004], unlike Paulson GIA model [*Paulson et al.*, 2007]. Peltier and Paulson models have been constructed assuming the same ice history and the same Earth internal structure, however they present a significant difference due to the way of treating the GIA-induced "rotational feedback" of the Earth. The GIA induces a component of the secular motion of the Earth's rotational axis, which in return creates an additional modification of the figure of the Earth due to the new inclination of the planet's elliptic bulge. This latter phenomenon is called the GIA rotational feedback [e.g., *Mitrovica et al.*, 2005; *Peltier and Luthcke*, 2009]. *Peltier and Luthcke* [2009] proposed that the recent ice melting (RIM) induced by recent climate change also generates a rotational feedback [see also *Mitrovica et al.*, 2009], which could explain differences between observations and GIA models.

[3] GIA and RIM also affect the long term evolution of the J_2 gravitational coefficient, which is linked to variations of oblateness of the Earth and the length of the day. It was been recognized that the J_2 trend ($\dot{J}_2$) has been globally negative for more than 30 years of Satellite Laser Ranging (SLR) observations, which is largely due to GIA [e.g., *Cheng et al.*, 2011]. Using SLR and GRACE data, a few recent studies propose a change in $\dot{J}_2$ sometime in the 1990s, probably due to recent global ice melting [*Roy and Peltier*, 2011; *Nerem and Wahr*, 2011]. All these observations ($\dot{J}_2$, rotational feedback) have been made using gravity measurements based on SLR or GRACE mission. Here we study rather independent data: global GNSS (Global Navigation Satellite System) velocities from the ITRF2008 global network [*Altamimi et al.*, 2011]. Surface velocity precise determination, the Earth's rotation, the mean sea level rise, satellite orbits, etc, fundamentally depend on the availability of a precise and stable reference frame. ITRF2008 is the up-to-date realization of the International Terrestrial Reference System (ITRS) that has been formally adopted and recommended for Earth science applications by the international community (IUGG2007 resolution number 2). In practice a reference frame is materialized by a compendium of station positions and velocities on a global network (see *Altamimi et al.* [2011] for more details). The ITRF2008 frame was constructed from a combination of global measurements based on reprocessed solutions of the four techniques of space geodesy. From the ITRF2008 GNSS vertical velocity subset, we inferred the degree-2 spherical harmonic coefficients (SHC) of the figure change of the Earth, that are directly linked to the Earth's oblateness, J_2 gravity rate, and rotation disruption. Note that studies have been done to

[1]Institut Géographique National, GRGS/LAREG, Marne-la-Vallée, France.
[2]Institut de Physique du Globe de Paris, Université Paris-Diderot, UMR 7154, Paris, France.

0094-8276/12/2011GL049942

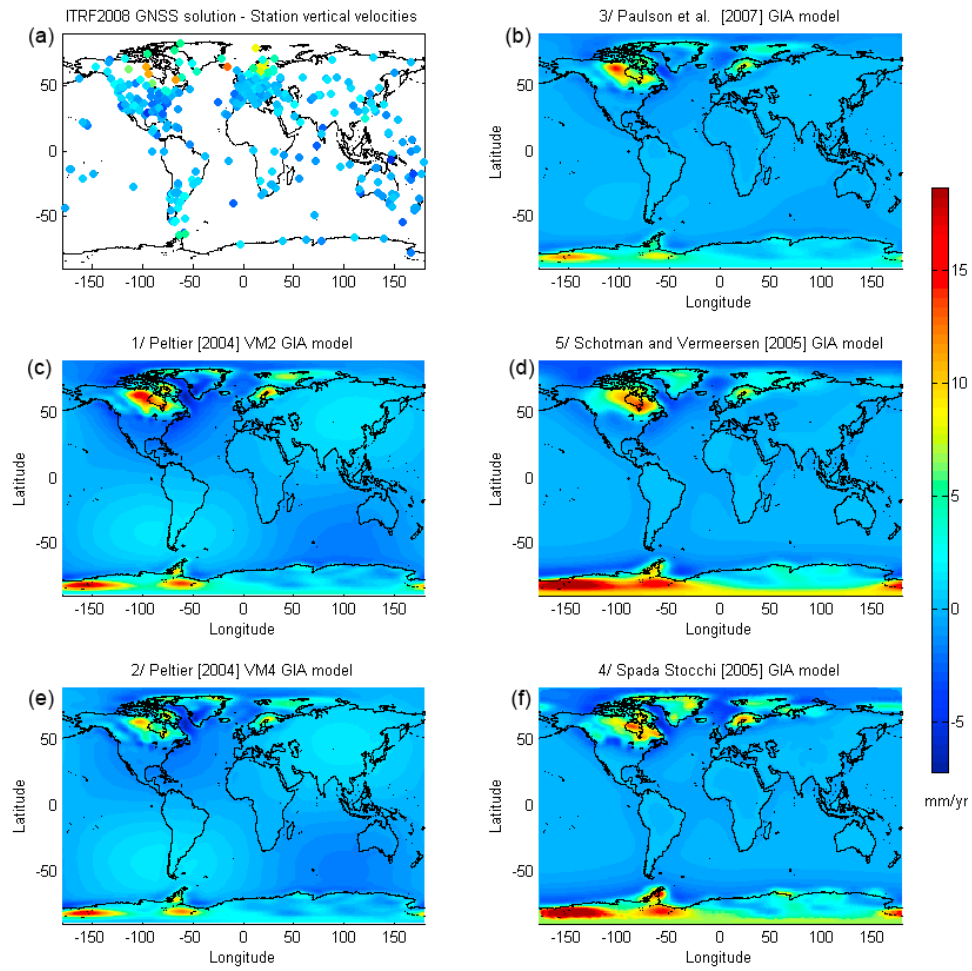

Figure 1. Ground vertical velocities: (a) from a core network of the ITRF2008-GNSS solution [*Altamimi et al.*, 2011], (b) from *Paulson et al.* [2007] GIA model, (c) from *Peltier* [2004] ICE5G-VM2 GIA model), (d) from *Schotman and Vermeersen* [2005] GIA model), (e) from *Peltier* [2004] ICE5G-VM4 GIA model), and (f) from *Spada and Stocchi* [2005] GIA model.

constrain GIA models using space geodetic data [e.g., *Argus and Peltier*, 2010; *Wu et al.*, 2010; *King et al.*, 2010, and references therein]. Some studies investigated denser geodetic networks than our network, particularly in GIA regions. On another hand, we use here the ITRF2008 solution, which has been shown to be far more accurate than previous ITRF solutions [*Altamimi et al.*, 2011].

[4] In the first part of the paper, the data used are detailed. In the second part, we describe our method: tests have been made with synthetic data in order to validate the method and to estimate realistic errors. In the last part, we present, analyze and discuss our results.

2. ITRF2008 Network and Observations

[5] Here we focus on the GNSS network of the ITRF2008 solution because of the present day high precision of the GNSS technique that benefited from a global reprocessing campaign and because the GNSS network is particularly dense [*Altamimi et al.*, 2011; *Collilieux et al.*, 2011]. The global ITRF2008-GNSS network contains 492 stations. In order to ensure the quality of the measurements, we only kept a core network of the most accurate station velocities that have been estimated with a higher precision than 0.35 mm/yr. However, we excluded a few stations that are well known to have non-unique velocity estimations in the ITRF solution due to large post-seismic disruptions. Finally, we excluded two stations that present very large subsidence due to local anthropogenic reasons (BOGT and INEG stations [*Blanco et al.*, 2010; *Esquivel et al.*, 2006]). Our selected network contains about 80% of the initial GNSS network. Figure 1a presents our GNSS station selection (on top) and their ITRF2008 vertical velocities. Stations that present the largest velocities are located in North America and Scandinavia, which enlightens the predominance of GIA signal in the ITRF2008-GNSS solution. It is quite clear when we compare it with predictions made by different GIA models (Figures 1b–1f). Nevertheless, one can see additional non zero vertical velocities on a few regions (Antarctica, Greenland and Iceland) that are larger in the ITRF2008 solution than in GIA models, suggesting the additional impact of RIM on these regions.

3. The Method, Error Estimation and GIA Models

[6] We calculated degree-2 SHC of surface vertical velocities using a general least square inversion by estimating

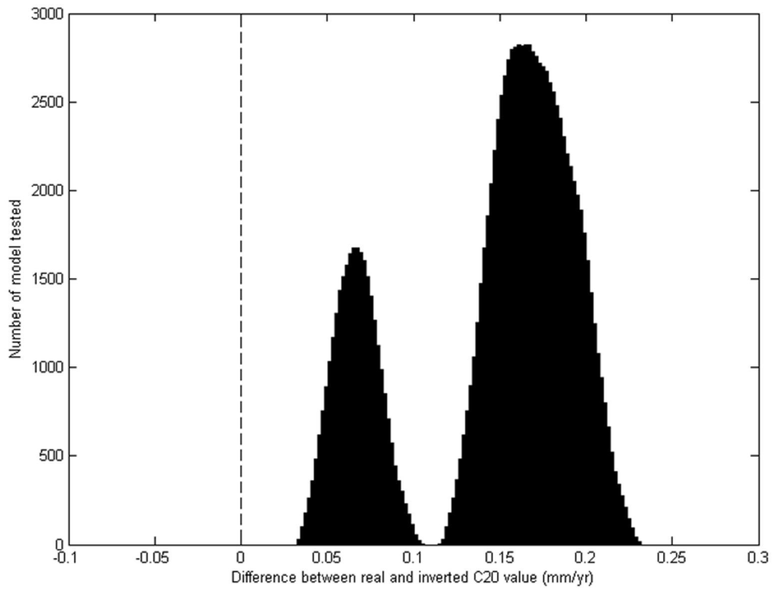

Figure 2. Inversion error in the degree-2 zonal spherical harmonic coefficients of the Earth's figure change (*C*20) obtained from synthetic tests on different GIA and RIM models. The estimation of *C*20 coefficient is always positively biased due to a lack of stations in the West Antarctica region.

low degrees altogether up to degree 5. The maximum degree has been chosen in order to minimize aliasing errors. Indeed, solving SHC for degree higher than 5–6 introduces particularly large errors in the estimation of degree-2 SHC, mostly due to the strong non-homogeneity of the station distribution in the network [e.g., *Wu et al.*, 2002] (see auxiliary material for more details).[1]

[7] It is well known that classical error estimations of such an inversion tend to be too optimistic. A reason is that the classical error estimation does not fully take into account the fact that high degrees are neglected and that geodetic networks are not well distributed over the globe. In order to test the method and to evaluate the quality of our inversion we investigated different GIA and RIM synthetic models. It offers the opportunity to statistically estimate realistic errors and to select the adapted parameters for such an inversion. We investigated the ICE5G-VM2 GIA model from *Peltier* [2004], Paulson GIA model [*Paulson et al.*, 2007] (models noted here after PE2 and PA), and three other GIA models: ICE5G-VM4 model also from Peltier (noted PE4), *Spada and Stocchi* [2005] model (noted SS), and *Schotman and Vermeersen* [2005] model (noted SV). The latter models have been constructed using different versions of the ice sheet history (including ICE3G and ICE4G) and/or different viscosity profiles. Note that SS and SV models do not take into account the rotational feedback. We also investigated simple RIM models in Greenland, Antarctica and glaciers around the world. The different models have been constructed following *Métivier et al.* [2010, 2011]. The ice sheet is considered to be melting uniformly in different regions (Greenland, West Antarctica, Alaska and other glaciers) with different rates that have been inferred from a set of published rate estimations from different authors (see *Métivier et al.* [2010, Figure 1] for more details). Note that a lot of these works give very different ice mass balances over the different regions, particularly over the Antarctica region (from −270 to −30 gigatons/yr in Greenland, from −300 to +100 gigatons/yr in Antarctica, etc). Exploring the entire set of possible RIM scenarios led us to construct a few thousand RIM models. We then tested the whole set of RIM models with each GIA model.

[8] We tested our inversion method with different parameters, e.g., with or without taking into account the full variance-covariance information from ITRF2008 stations. We finally chose to introduce no weighting in the inversion. The method is very sensitive to the station network shape and unfortunately variance-covariance weighting happens to slightly enhance the impact of the network heterogeneous distribution. For each degree-2 SHC, a maximum inversion error is estimated from the combination of all synthetic model inversions (based on the maximum differences between the SHC real values and their estimations).

[9] Stations close to the poles have a strong impact on the inversion of the degree 2 zonal SHC (noted *C*20). Therefore, stations on the Antarctica continent are for this reason critical for the inversion. Unfortunately, most Antarctican ITRF2008 stations are located in the East Antarctica region whereas the GIA signal is mostly over the West Antarctica region. For this reason the inversion of *C*20 coefficient tends to slightly over estimate the coefficient value and the error for this coefficient is larger than the other SHC. Figure 2 presents the difference between *C*20 estimations and real *C*20 for the synthetic models. Two Gaussian distributions can be seen in Figure 2 due to the different GIA models tested (left Gaussian form is due to SV model, the right one is due to the other combined models). For a given GIA model, the Gaussian distribution comes from the addition of all RIM models. We can see clearly that the difference between real and inverted *C*20 coefficients is always positive, due to Antarctica's lack of stations, for this reason the inverted *C*20 can be considered as an upper bound of the

[1]Auxiliary materials are available in the HTML. doi:10.1029/2011GL049942.

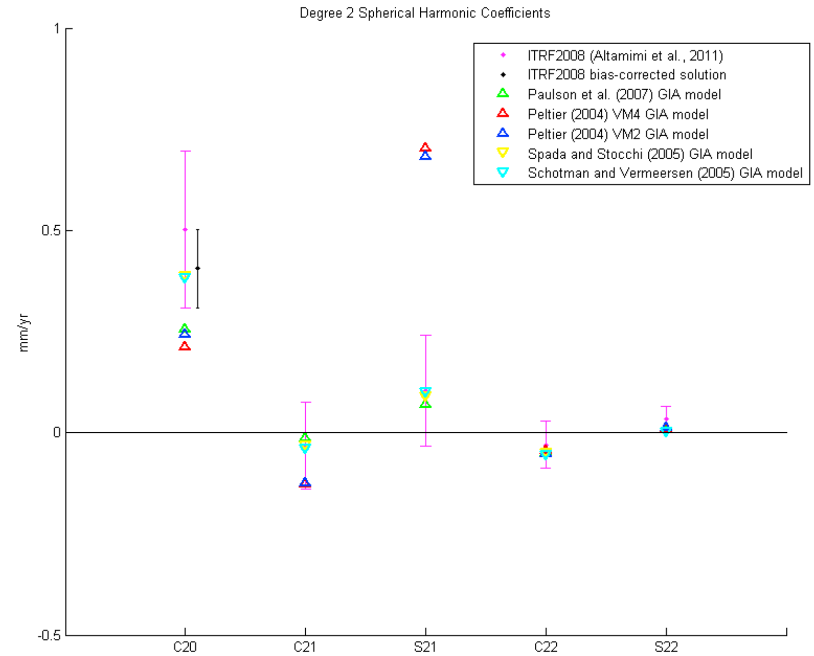

Figure 3. (a and b) Degree-2 spherical harmonic coefficients of ground station vertical velocities calculated from the ITRF2008-GNSS solution and different GIA models.

range of possible values. Note that we excluded the SS model from the error estimation because it gives an anomalously large error on the $C20$ SHC compared to other models due to particularly unrealistic station velocities on the eastern part of the Antarctica continent (see Figure 1). Indeed, the root mean square (RMS) of velocity differences between the ITRF2008 solution and SS model in Antarctica is two times larger than for the other models (around 4 mm/yr) (see Figure 1).

4. Results and Discussion

[10] The vertical velocity v of a station located at (θ,φ), where θ is the colatitude and φ the longitude, can be expressed as:

$$\mathrm{v}(\theta,\varphi) = C20\sqrt{5}\,\mathrm{P}_2^0(\cos\theta) + (C21\cos\varphi + S21\sin\varphi)\sqrt{\frac{5}{3}}\mathrm{P}_2^1(\cos\theta) + (C22\cos(2\varphi) + S22\sin(2\varphi))\sqrt{\frac{5}{12}}\mathrm{P}_2^2(\cos\theta) + \sum_{n\neq 2}\ldots \quad (1)$$

where the $\mathrm{P}_n^m(\cos\theta)$ are the associated Legendre polynomials of degree n and order m (note that spherical harmonics are normalized to 4π). We denote by $C20$ the SHC of degree 2 and order 0, $C21$ and $S21$ the cosine and sine SHC of degree 2 and order 1, and $C22$ and $S22$ the cosine and sine SHC of degree 2 and order 2. The five degree-2 terms of equation (1) characterize the very long wavelength of the Earth's figure change. The last sum represents all the other spherical harmonic terms with degree different than 2.

[11] Figure 3 shows our (C2m, S2m) estimation based on the ITRF2008-GNSS solution. The error bars correspond to the maximum errors observed in synthetic inversions. For $C20$, we also present a "bias-corrected solution" based on the fact that a lack of stations in West Antarctica positively biases the inversion (see section 3). We know that the $C20$ coefficient is always overestimated; therefore we may consider that the estimated $C20$ is the upper boundary of the $C20$ error bar. The real $C20$ should therefore be somewhere in the lower part of the initial error bar, which defines our "bias-corrected solution". Figure 3 also presents the theoretical value of degree-2 SHC of the different GIA models. We first see that our SHC globally present the same pattern as GIA model coefficients. As expected, we find coefficients $C22$ and $S22$ close to zero, which is consistent with all the models that we tested. For $C21$ and $S21$, we find values particularly close to all GIA models, except PE2 and PE4 models. These last two models show values respectively slightly and very different from our estimations (see the following discussion). Finally for $C20$, we find a large value that suggests a global decrease of oblateness of the Earth ($C20$ is related to oblateness with the opposite sign) that is stronger than $C20$ from PE2, PE4 and PA models.

[12] Actually, all our SHC are very close to the SHC from SS and SV models. But this similarity should be used cautiously. Indeed, ITRF2008 degree-2 SHC reflect, in theory, not only the GIA impact but also the impact of other phenomena such as recent climate changes. Assuming SS or SV model as a reference would mean that the RIM has a negligible impact on global geodetic parameters. In order to answer this question we investigated the $\dot{J}_2$ from our $C20$ estimations and compare with previous studies. The $\dot{J}_2$ coefficient is the non-dimensioned degree-2 zonal SHC of the geoid secular variation. It is of course linked to the oblateness of the Earth and consequently to our $C20$. However $\dot{J}_2$ and $C20$ are differently affected by GIA and RIM. Indeed, both phenomena tend to increase the $C20$, whereas they have opposite contributions on the $\dot{J}_2$. We investigate here what $\dot{J}_2$ the ITRF2008 solution suggests depending on the GIA model that we take into account. Let us consider

Table 1. $\dot{J}_2$ Estimations From GIA Models, ITRF2008 Solution and Recent Climate Changes[a]

GIA Model	$\dot{J}_2$ Induced by GIA ($\times 10^{-11}$)	$\dot{J}_2$ Induced by Recent Climate Changes ($\times 10^{-11}$)	$\dot{J}_2$ From ITRF2008 ($\times 10^{-11}$)[b]
Paulson et al. [2007]	−3.59	3.61 ± 2.37	0.02 ± 2.37
Peltier [2004] VM2	−4.02	3.97 ± 2.37	−0.05 ± 2.37
Peltier [2004] VM4	−3.40	5.76 ± 2.37	1.36 ± 2.37
Spada and Stocchi [2005]	−5.46	0.46 ± 2.37	−5.00 ± 2.37
Schotman and Vermeersen [2005]	−5.49	0.55 ± 2.37	−4.94 ± 2.37

[a]The $\dot{J}_2$ induced by recent climate change has been inferred from the gap between $C20^{ITRF}$ and $C20^{GIA}$ coefficients.
[b]Second column plus third column.

that the difference $C20^{ITRF} - C20^{GIA}$ is due to recent climate change. Then, based on elasto-gravitational theory we can calculate the RIM contribution to the $\dot{J}_2$, as follows:

$$\dot{J}_2^{RIM} = \sqrt{5}\,\frac{1 + k_2'}{h_2'}\,\frac{1}{a}\left(C20^{ITRF} - C20^{GIA}\right),$$

where k_2' and h_2' are the classical Love numbers [e.g., *Farrell*, 1972], and a Earth's mean radius. Knowing $\dot{J}_2^{GIA}$ from GIA models, we can then calculate $\dot{J}_2^{ITRF} = \dot{J}_2^{GIA} + \dot{J}_2^{RIM}$ for each GIA model. The results are summarized in Table 1 (third column). We see that ITRF2008 $C20$ induces a total $\dot{J}_2$ that is today close to zero if we assume PE2 or PA models, or largely negative if we assume SS or SV models. A few recent papers have shown that the J_2, based on SLR and GRACE observations, used to present a clear negative trend until sometime in the 1990s and then a still negative but close to zero trend [*Roy and Peltier*, 2011; *Nerem and Wahr*, 2011]. Since ITRF2008 has been constructed using GNSS measurement series from 1997.0 to 2009.5 and its origin has been constrained by SLR data spanning 1993.0 to 2009.0 [*Altamimi et al.*, 2011], our results should reflect the recent $\dot{J}_2$. If we consider PE2 and PA models, we effectively find a present $\dot{J}_2$ close to zero, suggesting a RIM contribution of approximately $(4.0 \pm 2.4) \times 10^{-11}$ yr^{-1} on $\dot{J}_2$. On the contrary SS and SV models today give $\dot{J}_2$ values (around $(-5 \pm 2.4) \times 10^{-11}$ yr^{-1}) that are not consistent with SLR and GRACE observations, even with the $\dot{J}_2$ before the 1990s (typically around -3×10^{-11} yr^{-1} [e.g., *Cheng and Tapley*, 2004; *Cheng et al.*, 2011; *Roy and Peltier*, 2011; *Nerem and Wahr*, 2011]).

[13] $C21$ and particularly $S21$ are the only coefficients impacted by the GIA rotational feedback [e.g., *Mitrovica et al.*, 2005]. In Figure 3, we see that $C21$ value of PE2 and PE4 models are slightly smaller than our $C21$ estimation but however within the range of possible values, considering the error estimation. $S21$ coefficients from PE2 and PE4 models are extremely large and our $S21$ estimation is closer to all the other GIA models, including SS and SV models that do not take into account the rotational feedback. Our results, based on the ITRF2008 solution and the global figure change of the Earth, tend to confirm GRACE observations and sea level rise assessments from *Chambers et al.* [2010] on the rotational feedback, i.e., a $S21$ very close to PA value (and other models) and a $S21$ from PE2 model extremely large (more than 7 times larger than our and PA values). Given the fact that PE2 and PA models are similar except for the rotational feedback calculation, this large gap in S21 is due to a very large rotational feedback in PE2 model. *Chambers et al.* [2010] concluded that PE2 is inconsistent with GRACE observations compared to PA model. We prefer to conclude that if PE2 model were to be correct, then we cannot explain our results except if RIM induces a particularly large rotational feedback that totally counteracts the GIA rotational feedback. On another hand, if we assume that PA model were to be correct, it means that GIA and RIM separately induce quite negligible rotational feedbacks. Both answers are extremes and call for more investigations on GIA model accuracy and rotational feedback.

[14] **Acknowledgments.** We thank Donald F. Argus and an anonymous reviewer for their helpful comments on the manuscript. We also thank Marianne Greff-Lefftz for fruitful discussions about Earth rotation. Four GIA models have been downloaded from the Special Bureau for Loading website (http://www.sbl.statkart.no/projects/pgs/ [*van Dam et al.*, 2002]). This is IPGP contribution XXXX.

[15] The Editor thanks James Davis and Donald Argus for their assistance in evaluating this paper.

References

Altamimi, Z., X. Collilieux, and L. Métivier (2011), ITRF2008: An improved solution of the international terrestrial reference frame, *J. Geod.*, *85*(8), 457–473, doi:10.1007/s00190-011-0444-4.

Argus, D. F. (2007), Defining the translational velocity of the reference frame of Earth, *Geophys. J. Int.*, *169*, 830–838, doi:10.1111/j.1365-246X.2007.03344.x.

Argus, D. F., and W. R. Peltier (2010), Constraining models of postglacial rebound using space geodesy: A detailed assessment of model ICE-5G (VM2) and its relatives, *Geophys. J. Int.*, *181*, 697–723, doi:10.1111/j.1365-246X.2010.04562.x.

Blanco, P., G. Barreto, and D. Ortiz (2010), *La Interferometría Diferencial DInSAR—Una Técnica Para el Monitoreo de la Subsidencia en Bogotá D.C.*, *Bol. Colomb. Geotec.*, vol. 13, Inst. Cartogr. de Catalunya, Barcelona, Spain.

Chambers, D. P., J. Wahr, M. E. Tamisea, and R. S. Nerem (2010), Ocean mass from GRACE and glacial isostatic adjustment, *J. Geophys. Res.*, *115*, B11415, doi:10.1029/2010JB007530.

Cheng, M., and B. D. Tapley (2004), Variations in the Earth's oblateness during the past 28 years, *J. Geophys. Res.*, *109*, B09402, doi:10.1029/2004JB003028.

Cheng, M., J. C. Ries, and B. D. Tapley (2011), Variations of the Earth's figure axis from satellite laser ranging and GRACE, *J. Geophys. Res.*, *116*, B01409, doi:10.1029/2010JB000850.

Collilieux, X., L. Métivier, Z. Altamimi, T. van Dam, and J. Ray (2011), Quality assessment of GPS reprocessed terrestrial reference frame, *GPS Solut.*, *15*(3), 219–231, doi:10.1007/s10291-010-0184-6.

Esquivel, R., A. Hernández, and M. Zermeño (2006), GPS for subsidence detection, the case study of Aguascalientes, in *Geodetic Deformation Monitoring: From Geophysical to Engineering Roles*, *IAG Symp.*, vol. 131, edited by F. Sanso and A. J. Gil, pp. 254–258, Springer, Berlin.

Farrell, W. E. (1972), Deformation of the Earth by surface loads, *Rev. Geophys.*, *10*(3), 761–797.

Greff-Lefftz, M. (2000), Secular variation of the geocenter, *J. Geophys. Res.*, *105*, 25,685–25,692, doi:10.1029/2000JB900224.

Greff-Lefftz, M., L. Métivier, and J. Besse (2010), Dynamic mantle density heterogeneities and global geodetic observables, *Geophys. J. Int.*, *180*, 1080–1094, doi:10.1111/j.1365-246X.2009.04490.x.

King, M., et al. (2010), Improved constraints on models of glacial isostatic adjustment. A review of the contribution of ground-based geodetic

observations, *Surv. Geophys.*, *31*(5), 465–507, doi:10.1007/s10712-010-9100-4.
Métivier, L., M. Greff-Lefftz, and Z. Altamimi (2010), On secular geocenter motion: The impact of climate changes, *Earth Planet. Sci. Lett.*, *296*, 360–366, doi:10.1016/j.epsl.2010.05.021.
Métivier, L., M. Greff-Lefftz, and Z. Altamimi (2011), Erratum to "On secular geocenter motion: The impact of climate changes" [Earth Planet. Sci. Lett. 296 (2010) 360–366], *Earth Planet. Sci. Lett.*, *306*, 136, doi:10.1016/j.epsl.2011.03.026.
Mitrovica, J. X., J. L. Davis, and I. I. Shapiro (1994), A spectral formalism for computing three-dimensional deformations due to surface loads: 2. Present-day glacial isostatic adjustment, *J. Geophys. Res.*, *99*(B4), 7075–7101, doi:10.1029/93JB03401.
Mitrovica, J. X., J. Wahr, I. Matsuyama, and A. Paulson (2005), The rotational stability of an ice-age Earth, *Geophys. J. Int.*, *161*, 491–506, doi:10.1111/j.1365-246X.2005.02609.x.
Mitrovica, J. X., N. Gomez, and P. U. Clark (2009), The sea-level fingerprint of West Antarctic collapse, *Science*, *323*, 753, doi:10.1126/science.1166510.
Nerem, R. S., and J. Wahr (2011), Recent changes in the Earth's oblateness driven by Greenland and Antarctic ice mass loss, *Geophys. Res. Lett.*, *38*, L13501, doi:10.1029/2011GL047879.
Paulson, A., S. Zhong, and J. Wahr (2007), Limitations on the inversion for mantle viscosity from postglacial rebound, *Geophys. J. Int.*, *168*, 1195–1209, doi:10.1111/j.1365-246X.2006.03222.x.
Peltier, W. R. (1974), The impulse response of a Maxwell Earth, *Rev. Geophys.*, *12*(4), 649–669.
Peltier, W. R. (1998), Postglacial variations in the level of the sea: Implications for climate dynamics and solid-Earth geophysics, *Rev. Geophys.*, *36*(4), 603–689.
Peltier, W. R. (2004), Global glacial isostasy and the surface of the Ice-Age Earth: The ICE-5G (VM2) model and GRACE, *Annu. Rev. Earth Planet. Sci.*, *32*, 111–149, doi:10.1146/annurev.earth.32.082503.144359.
Peltier, W. R., and S. B. Luthcke (2009), On the origins of Earth rotation anomalies: New insights on the basis of both "paleogeodetic" data and Gravity Recovery and Climate Experiment (GRACE) data, *J. Geophys. Res.*, *114*, B11405, doi:10.1029/2009JB006352.
Roy, K., and W. R. Peltier (2011), GRACE era secular trends in Earth rotation parameters: A global scale impact of the global warming process?, *Geophys. Res. Lett.*, *38*, L10306, doi:10.1029/2011GL047282.
Schotman, H. H. A., and L. L. A. Vermeersen (2005), Sensitivity of glacial isostatic adjustment models with shallow low-viscosity earth layers to the ice-load history in relation to the performance of GOCE and GRACE, *Earth Planet. Sci. Lett.*, *236*, 828–844, doi:10.1016/j.epsl.2005.04.008.
Spada, G., and P. Stocchi (2005), *Solving the "Sea Level Equation"—Part I: Theory*, Samizdat, Urbino, Italy.
Tapley, B. D., S. Bettadpur, J. C. Ries, P. F. Thompson, and M. M. Watkins (2004), GRACE measurements of mass variability in the Earth system, *Science*, *305*, 503–505, doi:10.1126/science.1099192.
van Dam, T., H.-P. Plag, O. Francis, and P. Gegout (2002), GGFC Special Bureau for Loading: Current status and plans, paper presented at IRES/GGFC Workshop, Int. Earth Rotation and Ref. Syst. Serv., Munich. [Available at http://www.sbl.statkart.no/archive/pos_paper_final.pdf.]
Wu, X., D. F. Argus, M. B. Heflin, E. Ivins, and F. H. Webb (2002), Site distribution and aliasing effects in the inversion for load coefficients and geocenter motion from GPS data, *Geophys. Res. Lett.*, *29*(24), 2210, doi:10.1029/2002GL016324.
Wu, X., M. B. Heflin, H. Schotman, L. L. A. Vermeersen, D. Dong, R. S. Gross, E. R. Ivins, A. W. Moore, and S. E. Owen (2010), Simultaneous estimation of global present-day water transport and glacial isostatic adjustment, *Nat. Geosci.*, *3*, 642–646, doi:10.1038/ngeo938.

Z. Altamimi, X. Collilieux, and L. Métivier, Institut Géographique National, GRGS/LAREG, 6-8 Avenue Blaise Pascal, F-77455 Marne-la-Vallée, France. (laurent.metivier@ign.fr)